School of Pharmaceutical Sciences[1]; Laboratory Animals Center[2], Sun Yat-sen University, Guangzhou, China

Resveratrol protects against triptolide-induced cardiotoxicity through SIRT3 signaling pathway *in vivo* and *in vitro*

Yanqin Yang[1], Wenwen Wang [1], Zhewen Xiong[1], Jiamin Kong[1], Li Wang[1], Yuwen Qiu[2], Feihai Shen[1], Zhiying Huang[1, 2]

Received March 18, 2016, accepted April 22, 2016

Zhiying Huang, Feihai Shen, School of Pharmaceutical Sciences, 132 East Circle at Higher Education Mega Center, Guangzhou 510006, P. R. China
hzhiying@mail.sysu.edu.cn (Z. Y. Huang)
tobyshum12@163.com (F. H. Shen)

Pharmazie 71 514–523 (2016) *doi: 10.1691/ph.2016.6597*

Clinical application of triptolide (TP), a main active ingredient of the traditional Chinese herb *Tripterygium wilfordii Hook f.* (TWHF), is limited by a series of severe toxicities, including cardiotoxicity. In previous studies, we found the activation of sirtuin 3 (SIRT3) attenuated TP-induced toxicity in cardiomyocytes. Resveratrol (RSV), a polyphenol from the skins of grapes and red wine, is an activator of SIRT3. The current study aimed to investigate the protective effect of RSV against TP-induced cardiotoxicity and the underlying mechanisms. Mice were treated with a single dose of TP (2.5 mg/kg) *via* the intragastric (i.g.) route. After 24 h, TP induced abnormal changes of serum biochemistry, activity decrease of antioxidant enzymes and damage of heart tissue such as myocardial fiber rupture, cell swelling and interstitial congestion. In contrast, administration with RSV (50 mg/kg i.g. 12 h before and 2 h after the administration of TP) attenuated the detrimental effects induced by TP in BALB/c mice. Moreover, the cardiomyocyte protective effects of RSV on TP-induced heart injury were associated with the activation of SIRT3 and its downstream targets. *In vitro* study also indicated that RSV counteracted TP-induced cardiotoxicity through SIRT3-FOXO3 signaling pathway in H9c2 cells. Collectively, these findings suggest the potential of RSV as a promising agent in protecting heart from TP-induced damage.

1. Introduction

Tripterygium wilfordii Hook f. (TWHF) has a long history of diverse uses in Traditional Chinese Medicines for its multiple bioactivities (Graziose et al. 2010). Triptolide (TP), the main ingredient of *Tripterygium wilfordii* is the major active component extracted from TWHF (Jin et al. 2015). However, 633 adverse reaction cases caused by *Tripterygium wilfordii* had been announced via CFDA (2004–2011.9), including 53 severe cases (Li et al. 2014b). It aroused concern to TP-induced severe toxicities that limited its clinical application (Kupchan et al. 1972). Among the adverse events, cardiotoxicity is non-negligible, even fatal (Guan et al. 2010; Fu 2004; Li et al. 2012). Studies revealed that TP-induced cardiac injury involved a mitochondria-dependent apoptosis pathway mediated by ROS. After TP treatment, the activities of antioxidant enzymes were reduced in dose-dependent and time-dependent manners. Accompanying with ROS augment, mitochondrial membrane potential ($\Delta\Psi m$) was depolarized while cytochrome c (Cyt C) was released into the cytosol (Zhou et al. 2014a). These results implied that mitochondrial permeability transition pore (mPTP) was involved in TP-induced heart injury. Furthermore, it was reported that TP decreased the oxidation of NADH into NAD^+, as the result of inhibition of complexes I and IV activities and blockage of electron flow in mitochondrial respiratory chain (Fu et al. 2011).

Sirtuin 3 (SIRT3), a NAD^+-dependent protein deacetylase with homology to the *Saccharomyces cerevisiae* gene silent information regulator 2 (Sir2), is the only member with direct link to extended lifespan of humans in sirtuins' family that includes 7 analogues (SIRT1~7) (Haigis and Guarente 2006). The heart protection of SIRT3 has been confirmed, attributing to its suppressive effects on cardiac hypertrophy and oxidative stress-mediated cardiomyocyte death (Pillai et al. 2010). SIRT3 deficiency promoted the phosphorylation of forkhead box class O transcription factor FOXO3 (Tseng et al. 2014), which resulted in the transcriptional down-regulation of manganese superoxide dismutase (Mn-SOD) and catalase (CAT) and caused ROS accumulation. Several proteins of mitochondrial energy metabolic enzymes such as complex I ~ V (Ahn et al. 2008; Koentges et al. 2015) were found obviously hyperacetylated in SIRT3-deficient mice. The heart contractility requires more energy than other organs. Factually, more than 90% energy in cardiomyocytes comes from mitochondrial respiration (Pillai et al. 2010). SIRT3 assists mitochondria to resist ROS impairment, balance energy homeostasis and maintain appropriate ATP level. Moreover, SIRT3 was investigated to deacetylate cyclophilin D (Cyp D) at lysine 166, followed by mPTP closing up (Hafner et al. 2010), and deacetylate Ku70, which prevented the departure of Bax from Ku70-Bax complex to mitochondria (Sundaresan et al. 2008). The effects above of SIRT3 prevent cells from Cyt C release, caspase-3 activation and subsequent apoptosis. Therefore, SIRT3 is crucial for maintaining heart normal function and repairing cardiomyocyte damage. In previous studies, SIRT3

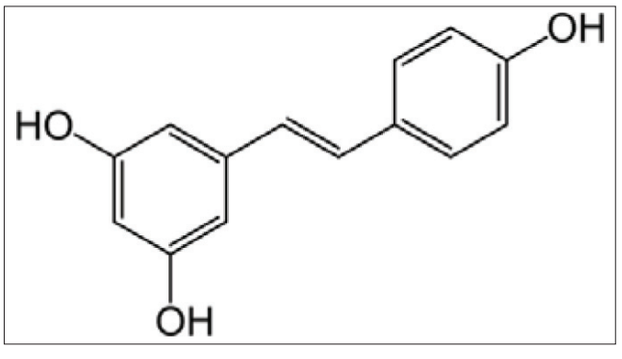

Fig. 1: Chemical structure of resveratrol

in H9c2 cells was upregulated as a stress-responsive factor both in nucleus and mitochondria after TP treatment. The SIRT3-FOXO3 signaling pathway was activated to eliminate ROS. The evidence of SIRT3 cardioprotection *in vitro* was supported by transient transfection with SIRT3 expression plasmid and SIRT3-siRNA.

Resveratrol (RSV, 3,5,4′-trihydroxystilbene), initially as a phytoalexin, is a member of the stilbene family from *grapevines*, *pines* and *legumes* (Fig. 1) (Burns et al. 2002). It was postulated to be the key constituent in red wine to exert cardioprotection in 1992. The positive roles of RSV in cardiovascular diseases have been reported

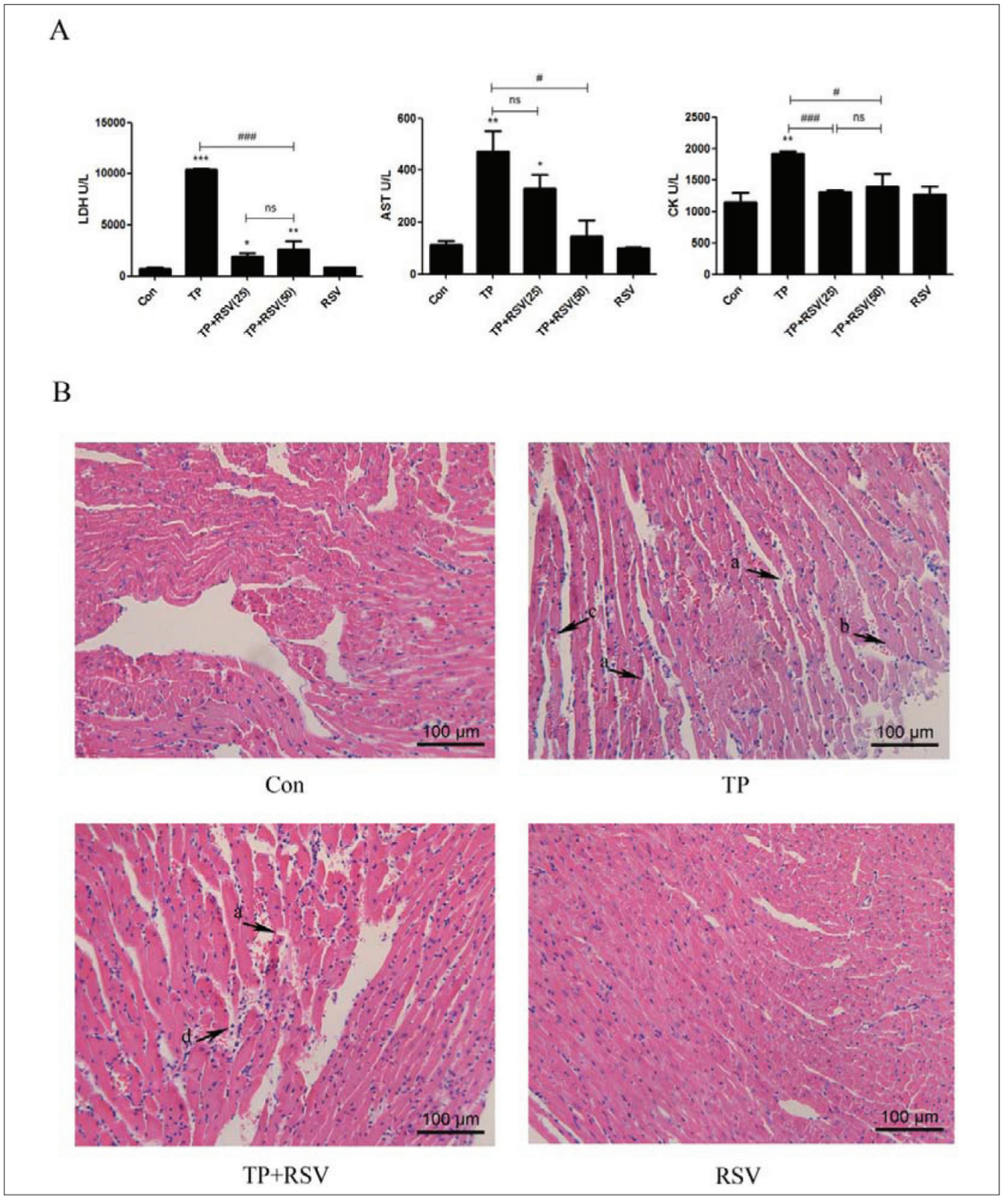

Fig. 2: Effects of RSV on TP-induced cardiotoxicity in BALB/c mice. All groups of BALB/c mice were treated via the i.g. route with distilled water, TP, TP plus RSV or RSV as the schedule. 24 h after TP administration, the mice were sacrificed. The effects of TP (2.5 mg/kg) and RSV (25,50 mg/kg) on the levels of LDH, AST, CK in serum were measured (A). The histological changes in mice heart tissues were observed by H&E staining (200 × magnification). As there were various lesions, letters were used to indicate the local lesion. a: myocardial fiber breakage; b: myocardial cell swelling; c: interstitial congestion; d: lymphocytic infiltration (B). Data are presented as the mean ± SD. *$p < 0.05$ vs. con., **$p < 0.01$ vs. con., ***$p < 0.001$ vs. con., #$p < 0.05$ vs. TP group, *ns* means no significance, n = 5.

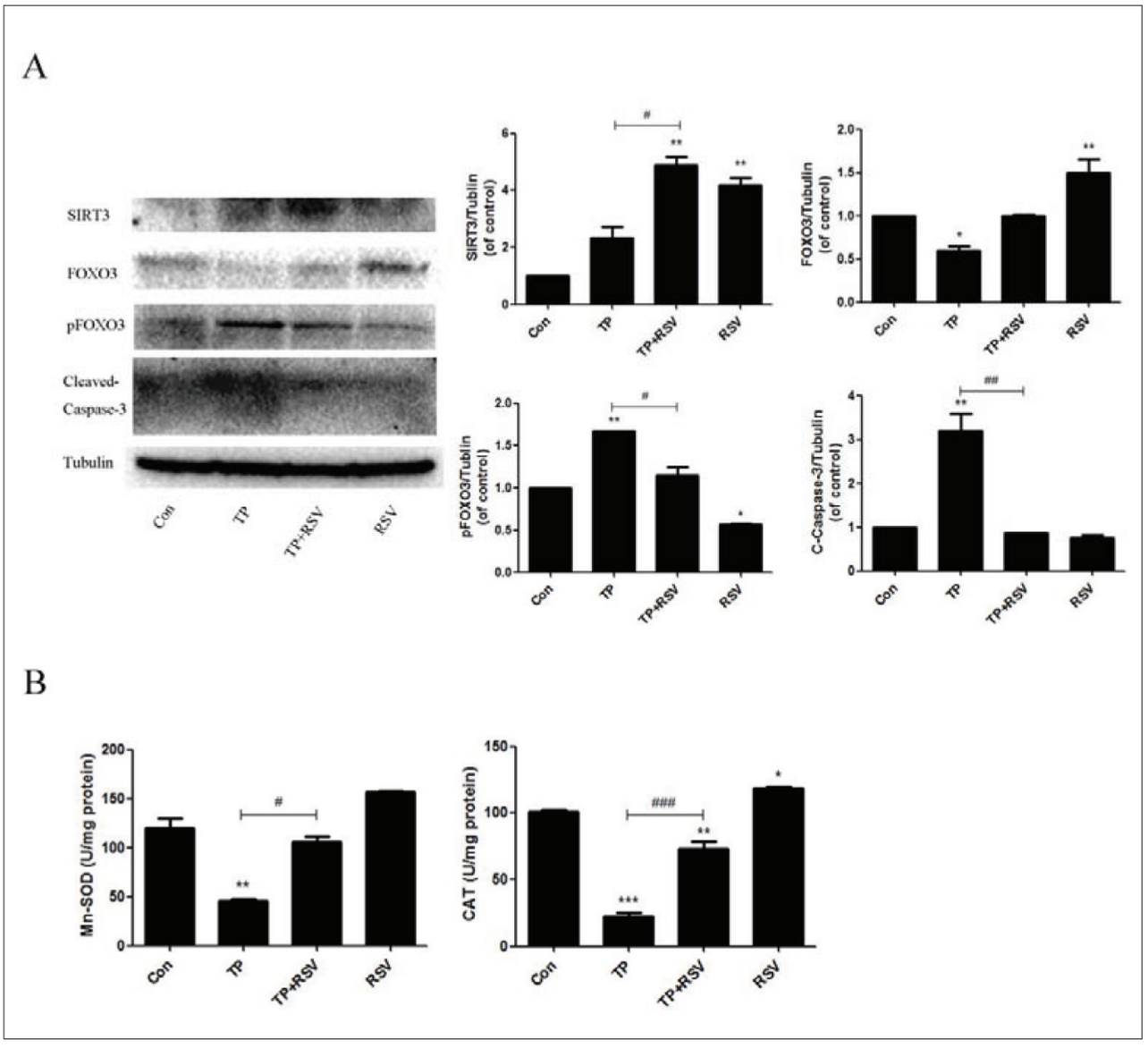

Fig. 3: Effects of RSV on SIRT3 pathway involved in TP-induced cardiotoxicity in BALB/c mice. All groups of BALB/c mice were respectively treated via i.g. route with distilled water, TP (2.5mg/kg), TP plus RSV (50 mg/kg) as the schedule. 24 h after TP administration. The protein levels of SIRT3, FOXO3, pFOXO3 and cleaved caspase-3 were assessed by Western blot (A). The activity of Mn-SOD and CAT were determined (B). Data are presented as the mean ± SD. *$p < 0.05$ vs. con., **$p < 0.01$ vs. con., ***$p < 0.001$ vs. con., #$p < 0.05$ vs. TP group, n = 5.

such as inhibiting platelet aggregation, promoting vasorelaxation, relieving atherosclerosis, reducing lipid peroxidation, regulating serum triglyceride and cholesterol concentrations (Baur and Sinclair 2006). RSV is absorbed well in human with nearly 70% absorptivity after oral consumption and it also undergoes rapid gastrointestinal absorption in mice. RSV was recently demonstrated as an activator of SIRT3 (Desquiret-Dumas et al. 2013; Zhou et al. 2014b) to alleviate cardiac fibrosis, prevent cardiac hypertrophy and improve cardiac function (Chen et al. 2015).

As a SIRT3 activator, the effect of RSV in TP-induced heart damage has not been evaluated before. Our present study targeted to depict the counteraction of RSV to TP-induced cardiotoxicity with BALB/c mice or H9c2 cells as a *in vivo* or a *in vitro* model, respectively. The protein levels of SIRT3, FOXO3, phosphorylated FOXO3 (pFOXO3) and activities of downstream antioxidant enzymes, Mn-SOD and CAT, were measured to explore the mechanisms of RSV protection. These findings suggested the potential of RSV as a promising agent for protecting heart against TP-induced damage and provided a possible strategy in clinical practice of TP.

2. Investigations and results

2.1. RSV reduced TP-induced cardiotoxicity in BALB/c mice

The effect of RSV on TP-induced cardiotoxicity was first evaluated *in vivo*. As shown in Fig. 2A, the activities of lactate dehydrogenase (LDH), aspartate aminotransferase (AST) and creatine kinase (CK) in TP-treated group increased 14.0-, 4.2- and 1.7-fold, respectively. In contrast, these indicators of cardiac injury were repressed by RSV (25 or 50 mg/kg) administration. Remarkably, the values of LDH were not significantly different between the group with 25 mg/kg RSV and the one with 50 mg/kg RSV, but the protection of RSV in 50 mg/kg dose was better than 25 mg/kg in active state and serum AST level. Therefore, the mice with RSV (50 mg/kg) treatment were used for the next experiments.

Histopathological analysis of the hearts (Fig. 2B) showed that no obvious abnormalities were observed in control group and RSV group. Myocardial fiber breakage, cell swelling and interstitial congestion were found in most of the mice exposed to TP alone.

However, these TP-induced heart injuries were repressed significantly by RSV treatment. These results indicated that RSV was able to protect against TP-induced cardiotoxicity in BALB/c mice.

2.2. *RSV activated the SIRT3-FOXO3 signaling pathway to protect cardiomyocytes in BALB/c mice*

To investigate the potential mechanism of RSV cardioprotection in BALB/c mice after TP treatment, we determined the protein levels of SIRT3, FOXO3, pFOXO3, cleaved caspase-3 by Western blot and the activity of Mn-SOD, CAT by commercial kits. It showed that the accumulation of FOXO3 was slightly lower in the hearts of TP-treated mice than that of the control mice (Fig. 3A), while the values of pFOXO3 and cleaved caspase-3 in the group treated with TP was dramatically higher than those in control group. However, we suggested that SIRT3 was not suppressed by TP. RSV activated the SIRT3-FOXO3 signaling pathway, which was characterized by upregulation of SIRT3, FOXO3 protein levels and downregulation of pFOXO3 protein level compared with control group. This function restored the protein expressions that were interfered by TP to the basal line as a result. Interestingly, RSV increased the SIRT3 expression after TP treatment to a higher level than control

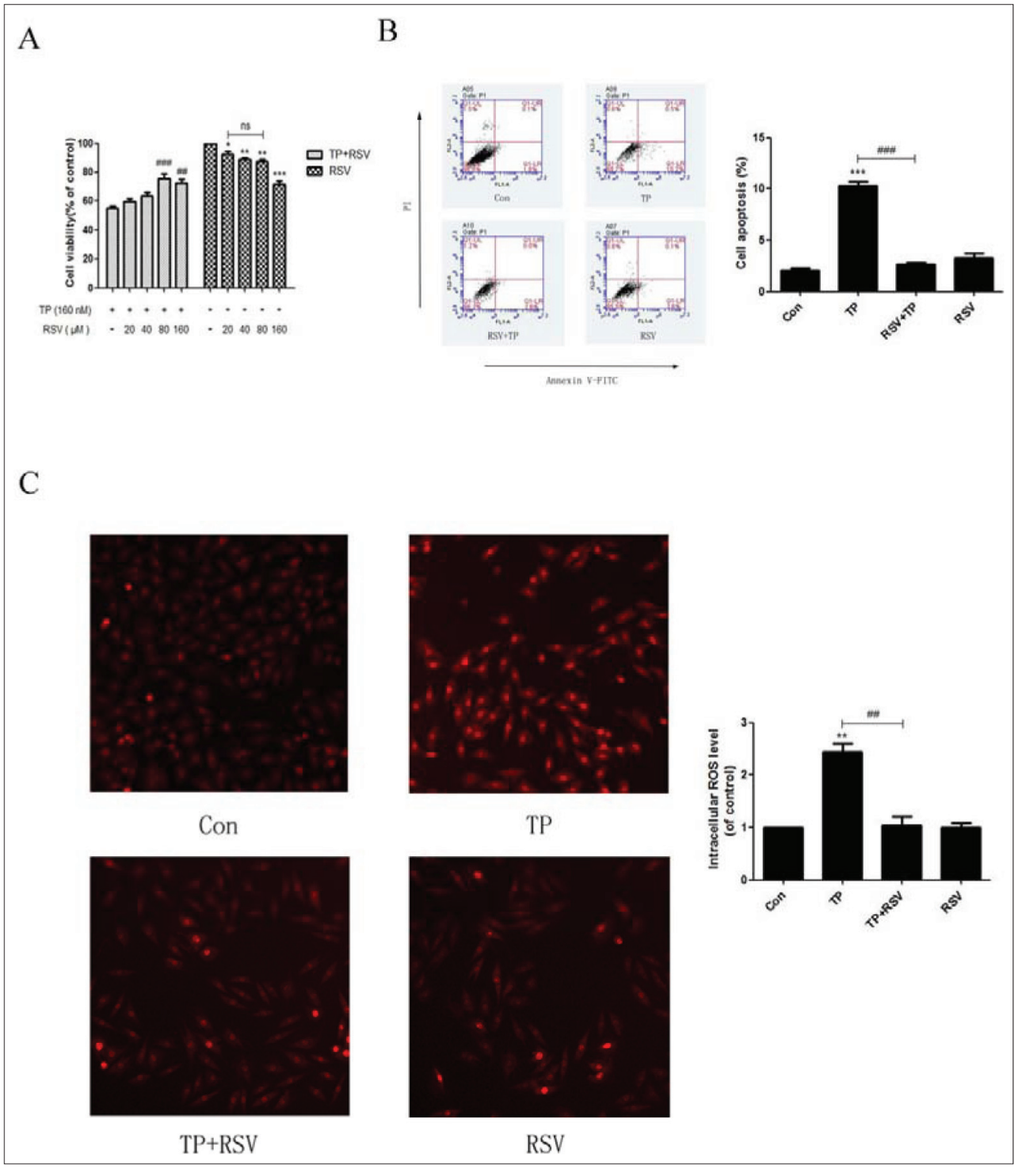

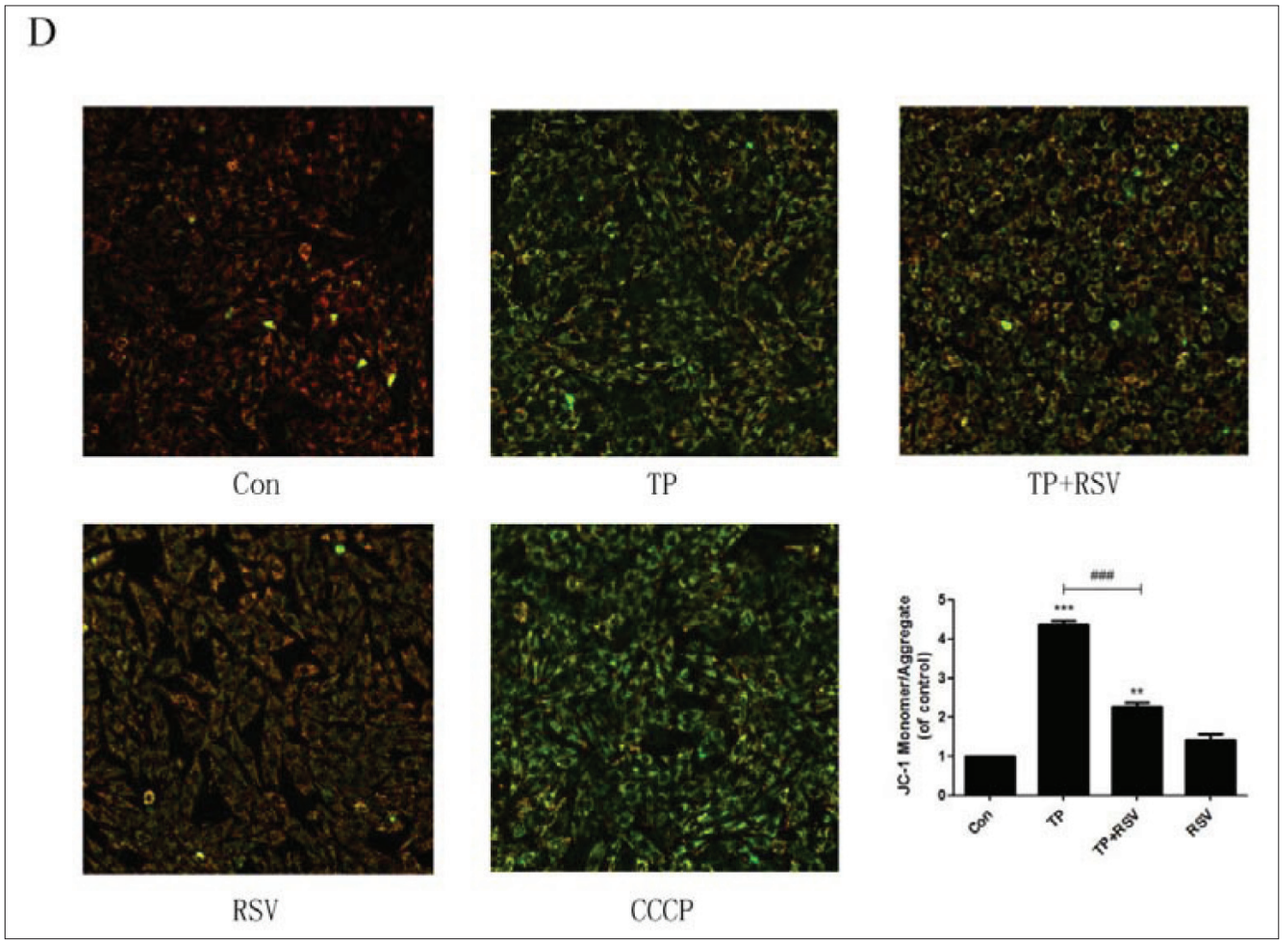

Fig. 4: Effects of RSV on TP-induced cytotoxicity in H9c2 cells. Cell viability was determined using MTT (A). Distributions of apoptotic cells were determined by Annexin V-FITC/PI double staining: Annexin V-positive/PI-negative, early apoptosis; Annexin V-positive/PI-positive, late apoptosis or necrosis (B). The ROS were detected using the fluorescent probe DHE (C). Representative pictures of JC-1 staining and quantitative analysis are shown (D). Carbonyl cyanide-m-chlorophenyl hydrazone (CCCP) was used as a positive control. Three independent experiments were conducted. Data are presented as the mean ± SD. *$p < 0.05$ vs. con., **$p < 0.01$ vs. con., ***$p < 0.001$ vs. con., #$p < 0.05$ vs. cells treated with the same concentration of TP, *ns* means no significance, n = 3.

group. Furthermore, upregulation of Mn-SOD and CAT enzymatic activity (Fig. 3B), two target genes of FOXO3, confirmed that the SIRT3-FOXO3 signaling pathway was activated by RSV as well. The results suggested that RSV increased activities of antioxidant enzymes to protect cardiomyocytes against ROS damage through SIRT3-FOXO3 signaling pathway in BALB/c mice.

2.3. *RSV reduced TP-induced cardiotoxicity in H9c2 cells*

The protective effects of RSV on cardiomyocytes *in vitro* were next determined. H9c2 cells were pretreated with RSV at various concentrations (20, 40, 80, 160 μM) for 6 h prior to TP treatment, and the toxicity of RSV was evaluated meanwhile with RSV treatment alone at corresponding concentrations. As shown in Fig. 4A, RSV at 160 μM reduced H9c2 cell viability notably, while the protection was no better than the one at 80 μM when co-treated with TP. We chose RSV (80 μM) as the protective agent against TP-induced cardiotoxicity in H9c2 cells with this reason. The amelioration of RSV to TP-induced cell apoptosis, ROS increase and ΔΨm depolarization was measured using annexin V-FITC/PI double-staining assay, DHE fluorescent probe and JC-1 staining, respectively. As we expected, RSV (80 μM) inhibited cell apoptosis (Fig. 4B), removed ROS aggregation (Fig. 4C) and reduced the loss of mitochondrial membrane potential (Fig. 4D) after cells were exposed to TP. These results indicated that RSV was able to protect against TP-induced cardiotoxicity in H9c2 cells.

2.4. *RSV activated SIRT3-FOXO3 signaling pathway to protect cardiomyocytes in H9c2 cells*

As it was suggested that RSV protected cardiomyocytes in BALB/c mice as a SIRT3 activator, the mechanisms of RSV protective effects related to SIRT3-FOXO3 signaling pathway on H9c2 cells were investigated subsequently. As shown in Fig. 5A, the SIRT3 level in total protein fraction (T-SIRT3) raised notably in cells treated with RSV and TP plus RSV. Compared with TP group, the level of total FOXO3 (T-FOXO3) increased in the group pretreated with RSV before TP treatment, though there was no statistical significance. However, TP plus RSV caused a significant reduction in FOXO3 acetylation, compared with TP treatment alone. Interestingly, RSV offset both SIRT3 (N-SIRT3) and FOXO3 (N-FOXO3) abatement in nuclear protein induced by TP, and suppressed the level of pFOXO3 in cytoplasm (P-pFOXO3) (Fig. 5B). There was no change of SIRT3 level in cytosolic proteins (P-SIRT3) after separating mitochondria from cells treated with RSV alone. When co-treated with TP-RSV, not only SIRT3 was activated dramatically in both mitochondrial (M-SIRT3) and cytosolic protein fractions (P-SIRT3), even exceeding that in RSV group, but also Cyt C release was depressed (Fig. 5C).
To verify the protective effect of RSV through activating SIRT3 protein, the SIRT3 gene was knocked down by siRNA-SIRT3 transfection before TP and RSV treatment. Fig. 6A shows that FOXO3 protein level decreased in cells transfected with siRNA-SIRT3 after TP treatment regardless of RSV existence. Furthermore, TP-induced changes in cellular morphology, such as bifurcating, shrinking and floating to the top of the media, were ameliorated by

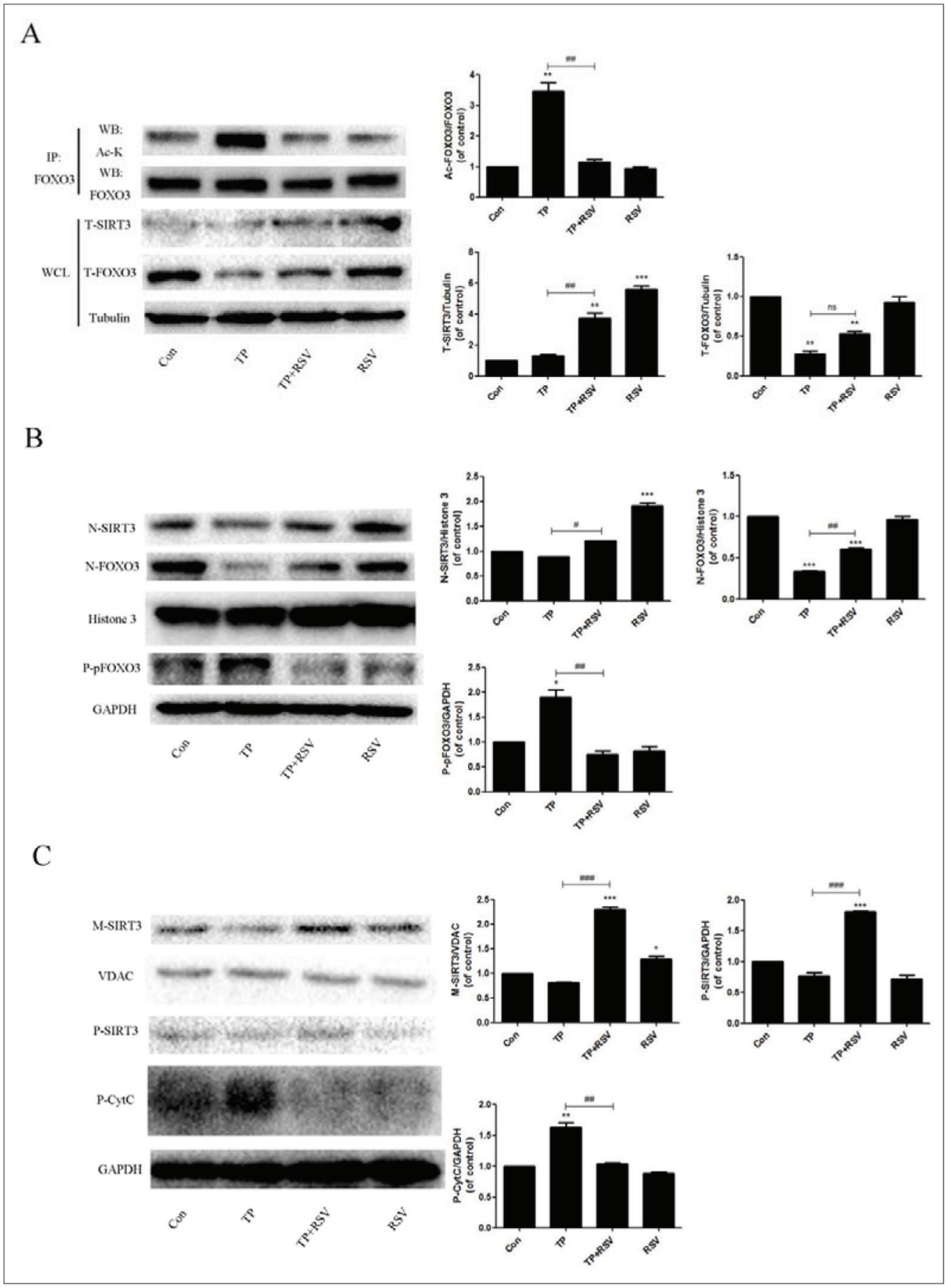

Fig. 5: Effects of RSV on the SIRT3 pathway involved in TP-induced cytotoxicity in H9c2 cells. H9c2 cells were pretreated with RSV (80 μM) for 6 h, then co-treated with TP (160 μM) and RSV (80 μM) for 24 h. The SIRT3 pathway related proteins were determined at total level (A), nuclear level (B) and mitochondrial level (C). Three independent experiments were conducted. Data are presented as the mean ± SD. *$p < 0.05$ vs. con., **$p < 0.01$ vs. con., ***$p < 0.001$ vs. con., #$p < 0.05$ vs. cells treated with the same concentration of TP, *ns* means no significance, n = 3.

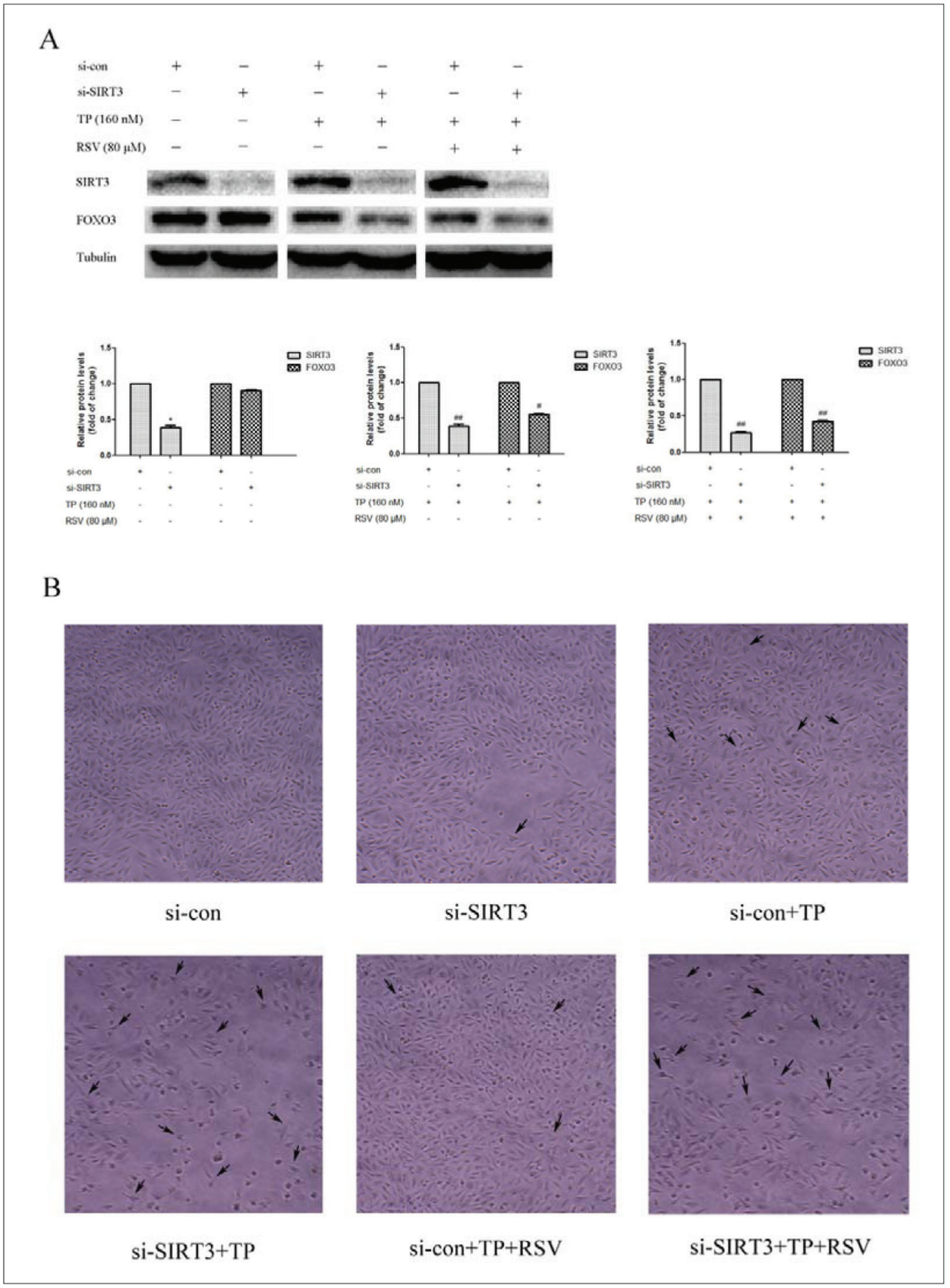

Fig. 6: Effects of RSV on TP-induced cytotoxicity in SIRT3 knockdown H9c2 cells. Pretreated with RSV for 6 h, then co-treated with TP and RSV for 24 h in siRNA-control or siRNA-SIRT3 transfected H9c2 cells, total levels of SIRT3, FOXO3 were assessed (A). Morphological changes in H9c2 cells after SIRT3 knockdown were observed under an inverted phase contrast microscope (100×, Olympus, Japan). The representative results from three independent experiments were shown (B). Data are presented as the mean ± SD. *$p < 0.05$ vs. con., **$p < 0.01$ vs. con., ***$p < 0.001$ vs. con., #$p < 0.05$ vs. cells treated with the same concentration of TP, *ns* means no significance, n = 3.

RSV in cells transfected with siRNA-control. These data indicated that RSV had little protective effect on H9c2 cells when SIRT3 gene was knocked down (Fig. 6B).

Taken together, we hypothesize that RSV, as an activator of SIRT3, mainly caused incremental SIRT3 protein translocation into nucleus during non-stress conditions. Redistribution of SIRT3 in TP plus RSV group meant that much of SIRT3 translocated from nucleus into mitochondria, which resulted from TP-induced cell stress. SIRT3 increased the level of activated FOXO3, the non-acetylated form, but not the total FOXO3 content. In other words, the residual SIRT3 in cytosol and nucleus assisted FOXO3 to reenter into nucleus from cytoplasm and remain there longer. These results indicated that RSV protected against TP-induced cardiotoxicity in H9c2 cells through both mitochondria- and nucleus-dependant SIRT3 signaling pathways.

3. Discussion

As one of the most powerful compounds with anti inflammatory/immunomodulatory action in TWHF, TP has therapeutic effect on organ-graft refection, autoimmune and inflammatory diseases (Wen et al. 2013). However, TP can also lead to severe cardiotoxicity and even death in therapeutic dose (Luo et al. 2009). In this study, we found that TP-induced an increase in cardiac enzyme activities (LDH, AST and CK), pathological lesions and the decrease of antioxidase activities were counteracted *in vivo*, while cell apoptosis, ROS augment, $\Delta\Psi m$ depolarization and morphological changes were resisted *in vitro* by RSV treatment. These results suggested that RSV could be used as a promising agent to protect the heart from TP-induced damage.

To explore the biological activities of RSV, doses from 0.1 mg/kg·bw (body weight) to 1000 mg/kg·bw were ever attempted in rodent models (Carrizzo et al. 2013). RSV has been employed for mitochondrial damage in lots of studies as a typical activator of SIRT1 (Lagouge et al. 2006; Yang et al. 2013). As the vital roles of SIRT3 in mitochondrial metabolism, integrity, genome maintenance, transcription and translation (Hebert et al. 2013) have been confirmed in eliminating ROS (Chang and Guarente 2014), the correlation between RSV and SIRT3 attracts much attention in maintaining cardiac health. Our study demonstrated that TP suppressed the activities of Mn-SOD and CAT, raised ROS accumulation and collapsed mitochondrial membrane potential *via* reducing the protein level of FOXO3 directly but not SIRT3. However, the TP-induced cardiotoxicity was alleviated after the activation of SIRT3 by RSV. We speculated SIRT3 participates in the protection against TP-induced myocardial damage but is not involved in the toxic mechanisms of TP. To prove if the increase of FOXO3 after RSV treatment was SIRT3-dependant, H9c2 cells were transfected with siRNA-SIRT3 to knock down the SIRT3 expression. It was seen that FOXO3 levels could not be upregulated and cell normal morphology could not be maintained by RSV without sufficient SIRT3 (Fig. 6). Interestingly, the expression of FOXO3 was not influenced by SIRT3 level under non-stress conditions, which implied that there was little interaction between SIRT3 and FOXO3 in normal physiological state. These results elucidated that RSV protected against TP-induced cardiotoxicity through the SIRT3 signaling pathway *in vivo* and *in vitro*.

Compared to the TP group, M-SIRT3, P-SIRT3 and N-FOXO3 increased remarkably, while P-pFOXO3 decreased notably in the TP plus RSV group. This pointed out that SIRT3, upregulated by RSV, played a protective role against TP-induced damage through both mitochondria- and nucleus-dependent signaling pathways. In mitochondria, according to previous reports, Cyp D was deacetyled by SIRT3 (Imaizumi et al. 2015) and mPTP closing up as a result of SIRT3 regulation (Bochaton et al. 2015). However, the inhibitory effects of mitochondrial gathered SIRT3 on mPTP after TP treatment needed further investigation. Acetylated FOXO3 was more susceptible to be phosphorylated and then exported from nucleus (Tseng et al. 2014) or degraded by proteasome (Sanchez et al. 2014). SIRT3 not only restrained the phosphorylation of FOXO3, but also improved the level of FOXO3 in nucleus and its downstream antioxidant enzymes, such as Mn-SOD and CAT, which resulted in prevention from ROS assault (Pantazi et al. 2013). As shown in Fig. 5A and 5B, the phenomenon that RSV increased SIRT3 expression without upregulating FOXO3 in RSV group was speculated that the level of SIRT3 did not affect FOXO3 under non-stress condition.

TP served as an anti-inflammatory and immunosuppressive agent through suppressing the expression of inducible nitric oxide synthase (iNOS), cyclooxygenase-2 (COX-2), interleukin 6 (IL-6), tumor necrosis factor α (TNF-α), the production of NO and the activation of nuclear factor κB (NF-κB) (Zhou et al. 2015). Overexpression of SIRT3 was reported to downregulate the phosphorylation of NF-κB (Song et al. 2014) so that we supposed the upregulation of SIRT3 by RSV would not weaken the anti-inflammation of TP. Additionally, the anti-inflammatory activity of RSV is usually associated to inhibition of TNF-α-mediated NF-κB inflammatory pathways, in which iNOS, IL-6, activator protein-1 (AP-1) and COX-2 act as inflammatory markers (Csiszar et al. 2006; Manna et al. 2000; de la Lastra and Villegas 2005; Neves et al. 2012). Therefore, RSV is suggested to enhance the anti-inflammatory effects of TP while attenuating TP-induced cardiotoxicity.

In summary, the results obtained in this study revealed a protective role of RSV against TP-induced cardiotoxicity *in vivo* and *in vitro*. This protection was realized possibly *via* the activation of SIRT3-FOXO3 signaling pathways. The findings imply the potential of RSV for preventing and treating TP-induced cardiotoxicity in the clinical application of TP.

4. Experimental

4.1. Materials and reagents

TP (>99% purity) was purchased from DND Pharm-Technology Co. (Shanghai, China). RSV (>99% purity) was purchased from Sigma–Aldrich (St. Louis, MO, USA). MTT were purchased from MP Biomedicals (Santa Ana, CA, USA). Anti-SIRT3 antibody, anti-FOXO3 antibody, anti-acetylated-lysine antibody, anti-caspase-3 antibody, anti-VDAC antibody and anti-histone H3 antibody were purchased from Cell Signaling Technology (Beverly, MA, USA). Anti-pFOXO3 antibody was purchased from ABclonal Technology (Cambridge, MA, USA). The reagents used for measuring the activities of Mn-SOD and CAT were purchased from Beyotime (Shanghai, China). Cell culture materials were purchased from NEST Biotech (Jiangsu, China). All chemicals were of analytical grade.

4.2. Animals and treatment

Both male and female BALB/c mice (6 weeks) were purchased from the Laboratory Animal Center of Sun Yat-sen University, Guangzhou, China. All mice were fed in a specific pathogen-free animal facility under a 12-h light–dark alternation at a temperature of 23±3 °C and humidity of 55±15 %. Food and water without pathogen were provided ad libitum. All of the animal experimental protocols in this study were performed in accordance with the guidelines approved by the Animal Ethical and Welfare Committee of Sun Yat-sen University (Approval No: IACUC-DD-15-0802).

To examine the role of RSV in TP-induced cardiotoxicity, all mice were randomized to the following 4 groups: (1) control group, (2) TP group: mice were treated with 2.5 mg/kg TP i.g. for one administration, (3) TP plus RSV group: mice were treated intragastricly with RSV (50 mg/kg) at 12 h before and 2 h after TP (2.5mg/kg) administration, (4) RSV group: mice were treated with 50 mg/kg RSV i.g. administration. All mice in this study were anesthetized 24 h after TP treatment. Blood and heart samples were collected according to Zhou et al. (2015) for further analysis.

4.3. Serum biochemical assay

Levels of cardiac enzymes, LDH, AST and CK, in serum were measured to evaluate the physiological functions, using commercially available enzymatic assay kits (Leadman Group Co., Ltd., Beijing, China).

4.4. Histopathological examinations

Heart from each mouse was cut apart and immersed individually in a formaldehyde solution for 24 h. The formaldehyde solution comprised 10% of a 37–40% formaldehyde and 90% of a 0.01 mol/L PBS (pH 7.4). After embedded in paraffin, sections were cut at 3 μM and stained with hematoxylin-eosin for histological evaluation.

4.5. Determination of Mn-SOD and CAT

Activities of Mn-SOD and CAT in homogenized heart were measured using commercial kits (Beyotime, Shanghai, China) according to the manufacturer's instructions.

4.6. Cell culture and drug dissolution

H9c2 cells, obtained from the American Type Culture Collection (ATCC, USA), were cultured in Dulbecco's modified Eagle's medium (DMEM, HyClone, Logan, UT, USA) complemented with 10% fetal bovine serum (FBS, HyClone, Logan, UT, USA) and 1% antibiotics of penicillin/streptomycin. Cells were cultured in a humidified incubator with 5% CO_2 at 37 °C. TP and RSV were dissolved in DMSO to make stock solutions which were stored stably at -20°C.

4.7. MTT assay

A total of 4×10^3 H9c2 cells were seeded into a well of 96-well plates. After incubation at 37 °C for 24 h, cells were treated with TP and RSV. Cell viability was measured by a 3-(4,5-dimethylthiazol-2-yl)-2,5-diphenyl tetrazolium bromide (MTT) assay as Li reported (Li et al. 2014a).

4.8. Detection of apoptosis

A total of 4×10^4 H9c2 cells were seeded into a well of 6-well plates and treated with TP and RSV. Cell apoptosis was determined using flow cytometry (Becton Dickinson, San Jose, CA, USA) with Annexin V-FITC Apoptosis Detection kit (KeyGEN Biotech, Jiangsu, China) in accordance with the manufacturer's instructions.

4.9. Determination of ROS production

Intracellular accumulation of ROS was determined by fluorescent probe DHE using the ROS Detection Kit (Beyotime, Shanghai, China). A total of 1×10^4 H9c2 cells were seeded into a well of 24-well plates and exposed to TP and RSV. Twenty-four hours later, fluorescence was photographed immediately in high contend screening (ArrayScanVTI, Thermo Fisher, USA).

4.10. Measurement of $\Delta\Psi m$

A total of 1×10^4 H9c2 cells were seeded into a well of 24-well plates. After exposure to TP and RSV, mitochondrial $\Delta\Psi m$ was determined by JC-1 fluorescence intensity using JC-1 Detection Kit (Beyotime, Shanghai, China) in High Contend Screening (ArrayScanVTI, Thermo Fisher, USA) at a single excitation wavelength (488 nm) and dual emission wavelengths (shift from 530 nm to 590 nm).

4.11. Immunoprecipitation of acetyl lysine-modified FOXO3

H9c2 cells were treated with Cell Protein Extraction Reagent (Beyotime, Shanghai, China) and protease inhibitor cocktail (Merck, Darmstadt, Germany). Cell extracts were lysed on the ice for 30 min and centrifuged at 10000 g at 4 for 20 min. The protein concentration was determined using the BCA Protein Assay kit (Pierce Chemical Co., Rockford, USA). 200 µg of total proteins was incubated with anti-FOXO3 antibody overnight. Then, 40 µL of protein A/G-agarose (Beyotime, Shanghai, China) was added and incubated at 4°C for 4 h. Pellets were centrifuged for further analysis by SDS-PAGE.

4.12. Western blot analysis

Heart tissue were disintegrated by electric homogenizer and lysed on ice with T-PER Tissue reagent, while H9c2 cells were treated with Cell Protein Extraction Reagent (Pierce Chemical Co., Rockford, USA), to extract the total protein. Nuclear protein fraction was prepared using a Nuclear Extract kit (Active Motif, Carlsbad, CA, USA), as the mitochondrial protein fraction using a Mitochondria Isolation Kit (Beyotime, Shanghai, China), in accordance with the manufacturer's instructions. Western blot analysis was completed as previously reported (Li et al. 2014a).

4.13. Statistical analysis

SPSS v16.0 software (SPSS Inc., Chicago, IL, USA) was used for statistical analysis. The statistics were expressed as the mean ± S.D. Statistical comparisons were made via Student's t-test and oneway analysis of variance (ANOVA), followed by Tukey's test. The level of significance was set at $p < 0.05$, $p < 0.01$ or $p < 0.001$.

Acknowledgements: This study was supported by the General Projects in the National Natural Science Foundation of China (Grant No. 81473416) and Guangdong Province Scientific Program Project (2012B060300016), and all support is gratefully acknowledged.

Conflict of interest: The authors have declared no conflict of interest.

References

Ahn BH, Kim HS, Song S, Lee IH, Liu J, Vassilopoulos A, Deng CX, Finkel T (2008) A role for the mitochondrial deacetylase Sirt3 in regulating energy homeostasis. Proc Natl Acad Sci USA 105: 14447-14452.

Baur JA, Sinclair DA (2006) Therapeutic potential of resveratrol: the *in vivo* evidence. Nat Rev Drug Discov 5: 493-506.

Bochaton T, Crola-Da-Silva C, Pillot B, Villedieu C, Ferreras L, Alam MR, Thibault H, Strina M, Gharib A, Ovize M, Baetz D (2015). Inhibition of myocardial reperfusion injury by ischemic postconditioning requires sirtuin 3-mediated deacetylation of cyclophilin D. J Mol Cell Cardiol 84: 61-69.

Burns J, Yokota T, Ashihara H, Lean ME, Crozier A (2002). Plant foods and herbal sources of resveratrol. J Agric Food Chem 50: 3337-3340.

Carrizzo A, Forte M, Damato A, Trimarco V, Salzano F, Bartolo M, Maciag A, Puca AA, Vecchione C (2013). Antioxidant effects of resveratrol in cardiovascular, cerebral and metabolic diseases. Food Chem Toxicol 61: 215-226.

Chang HC, Guarente L (2014) SIRT1 and other sirtuins in metabolism. Trends Endocrinol Metab 25: 138-145.

Chen T, Li J, Liu J, Li N, Wang S, Liu H, Zeng M, Zhang Y, Bu P (2015) Activation of SIRT3 by resveratrol ameliorates cardiac fibrosis and improves cardiac function via the TGF-beta/Smad3 pathway. Am J Physiol Heart Circ Physiol 308: H424-434.

Csiszar A, Smith K, Labinskyy N, Orosz Z, Rivera A, Ungvari Z (2006) Resveratrol attenuates TNF-alpha-induced activation of coronary arterial endothelial cells: role of NF-kappaB inhibition. Am J Physiol Heart Circ Physiol 291: H1694-1699.

de la Lastra CA, Villegas I (2005) Resveratrol as an anti-inflammatory and anti-aging agent: mechanisms and clinical implications. Mol Nutr Food Res 49: 405-430.

Desquiret-Dumas V, Gueguen N, Leman G, Baron S, Nivet-Antoine V, Chupin S, Chevrollier A, Vessieres E, Ayer A, Ferre M, Bonneau D, Henrion D, Reynier P, Procaccio V (2013) Resveratrol induces a mitochondrial complex I-dependent increase in NADH oxidation responsible for sirtuin activation in liver cells. J Biol Chem 288: 36662-36675.

Fu BH (2004) Severe toxic effects of the whole grass and roots of Tripterygium wilfordii Hook f. (TWHF), with three clinical cases of TWHF on acute toxic myocarditis attached. Fourth Natl. Conf. Proc. TWHF 456 (in Chinese).

Fu Q, Huang X, Shu B, Xue M, Zhang P, Wang T, Liu L, Jiang Z, Zhang L (2011) Inhibition of mitochondrial respiratory chain is involved in triptolide-induced liver injury. Fitoterapia 82: 1241-1248.

Graziose R, Lila MA, Raskin I (2010) Merging traditional Chinese medicine with modern drug discovery technologies to find novel drugs and functional foods. Curr Drug Discov Technol 7: 2-12.

Guan W, Dai QB, Hu YL, Zhang W, Hua ZJ (2010) Myocardial toxicity of triptolide on rats: the temporal rhythm effect. J Wannan Med Univ 29: 18–21.

Hafner AV, Dai J, Gomes AP, Xiao CY, Palmeira CM, Rosenzweig A, Sinclair DA (2010) Regulation of the mPTP by SIRT3-mediated deacetylation of Cyp D at lysine 166 suppresses age-related cardiac hypertrophy. Aging (Albany NY) 2: 914-923.

Haigis MC, Guarente LP (2006) Mammalian sirtuins--emerging roles in physiology, aging, and calorie restriction. Genes Dev 20: 2913-2921.

Hebert AS, Dittenhafer-Reed KE, Yu W, Bailey DJ, Selen ES, Boersma MD, Carson JJ, Tonelli M, Balloon AJ, Higbee AJ, Westphall MS, Pagliarini DJ, Prolla TA, Assadi-Porter F, Roy S, Denu JM, Coon JJ (2013) Calorie restriction and SIRT3 trigger global reprogramming of the mitochondrial protein acetylome. Mol Cell 49: 186-199.

Imaizumi N, Kwang Lee K, Zhang C, Boelsterli UA (2015) Mechanisms of cell death pathway activation following drug-induced inhibition of mitochondrial complex I. Redox Biol 4: 279-288.

Jin J, Sun X, Zhao Z, Wang W, Qiu Y, Fu X, Huang M, Huang Z (2015) Activation of the farnesoid X receptor attenuates triptolide-induced liver toxicity. Phytomedicine 22: 894-901.

Koentges C, Pfeil K, Schnick T, Wiese S, Dahlbock R, Cimolai MC, Meyer-Steenbuck M, Cenkerova K, Hoffmann MM, Jaeger C, Odening KE, Kammerer B, Hein L, Bode C, Bugger H (2015) SIRT3 deficiency impairs mitochondrial and contractile function in the heart. Basic Res Cardiol 110: 36.

Kupchan SM, Court WA, Dailey RG Jr., Gilmore CJ, Bryan RF (1972) Triptolide and tripdiolide, novel antileukemic diterpenoid triepoxides from Tripterygium wilfordii. J Am Chem Soc 94: 7194-7195.

Lagouge M, Argmann C, Gerhart-Hines Z, Meziane H, Lerin C, Daussin F, Messadeq N, Milne J, Lambert P, Elliott P, Geny B, Laakso M, Puigserver P, Auwerx J (2006) Resveratrol improves mitochondrial function and protects against metabolic disease by activating SIRT1 and PGC-1alpha. Cell 127: 1109-1122.

Li H, Qiu Y, Tang N, Wang X, Song Z, Zhou G, Ma J (2012) Study on cardiac toxicity of *Tripterygium wilfordii*. Proceedings of the first Annual Conference on Drug Toxicology of China and the International Symposium on non clinical safety evaluation: 157-158.

Li J, Shen F, Guan C, Wang W, Sun X, Fu X, Huang M, Jin J, Huang Z (2014a) Activation of Nrf2 protects against triptolide-induced hepatotoxicity. PLoS One 9: e100685.

Li XJ, Jiang ZZ, Zhang LY (2014b) Triptolide: progress on research in pharmacodynamics and toxicology. J Ethnopharmacol 155: 67-79.

Luo Y, Shi C, Yuan Y, Zhang M, Liao M (2009). Advances in researches on the toxicology of triptolide. J Toxicol 23: 74-77.

Manna SK, Mukhopadhyay A, Aggarwal BB (2000) Resveratrol suppresses TNF-induced activation of nuclear transcription factors NF-κB, activator protein-1, and apoptosis: potential role of reactive oxygen intermediates and lipid peroxidation. J Immunol 164: 6509-6519.

Neves AR, Lucio M, Lima JL, Reis S (2012). Resveratrol in medicinal chemistry: a critical review of its pharmacokinetics, drug-delivery, and membrane interactions. Curr Med Chem 19: 1663-1681.

Pantazi E, Zaouali MA, Bejaoui M, Folch-Puy E, Ben Abdennebi H, Rosello-Catafau J (2013) Role of sirtuins in ischemia-reperfusion injury. World J Gastroenterol 19: 7594-7602.

Pillai VB, Sundaresan NR, Jeevanandam V, Gupta MP (2010) Mitochondrial SIRT3 and heart disease. Cardiovasc Res 88: 250-256.

Sanchez AM, Candau RB, Bernardi H (2014) FoxO transcription factors: their roles in the maintenance of skeletal muscle homeostasis. Cell Mol Life Sci 71: 1657-1671.

Song Y, Shi J, Wu Y, Han C, Zou J, Shi Y, Liu Z (2014) Metformin ameliorates insulin resistance in L6 rat skeletal muscle cells through upregulation of SIRT3. Chin Med J (Engl) 127: 1523-1529.

Sundaresan NR, Samant SA, Pillai VB, Rajamohan SB, Gupta MP (2008) SIRT3 is a stress-responsive deacetylase in cardiomyocytes that protects cells from stress-mediated cell death by deacetylation of Ku70. Mol Cell Biol 28: 6384-6401.

Tseng AH, Wu LH, Shieh SS, Wang DL (2014) SIRT3 interactions with FOXO3 acetylation, phosphorylation and ubiquitinylation mediate endothelial cell responses to hypoxia. Biochem J 464: 157-168.

Wen HL, Liang ZS, Zhang R, Yang K (2013) Anti-inflammatory effects of triptolide improve left ventricular function in a rat model of diabetic cardiomyopathy. Cardiovasc Diabetol 12: 50.

Yang Y, Duan W, Lin Y, Yi W, Liang Z, Yan J, Wang N, Deng C, Zhang S, Li Y, Chen W, Yu S, Yi D, Jin Z (2013) SIRT1 activation by curcumin pretreatment attenuates mitochondrial oxidative damage induced by myocardial ischemia reperfusion injury. Free Radic Biol Med 65: 667-679.

Zhou J, Xi C, Wang W, Fu X, Jinqiang L, Qiu Y, Jin J, Xu J, Huang Z (2014a) Triptolide-induced oxidative stress involved with Nrf2 contribute to cardiomyocyte apoptosis through mitochondrial dependent pathways. Toxicol Lett 230: 454-466.

Zhou J, Xi C, Wang W, Yang Y, Qiu Y, Huang Z (2015) Autophagy plays an important role in triptolide-induced apoptosis in cardiomyocytes. Toxicol Lett 236: 168-183.

Zhou X, Chen M, Zeng X, Yang J, Deng H, Yi L, Mi MT (2014b) Resveratrol regulates mitochondrial reactive oxygen species homeostasis through Sirt3 signaling pathway in human vascular endothelial cells. Cell Death Dis 5: e1576.